Biophysical Journal Volume 100 April 2011 1960–1968

# Increasing Hydrophobicity of Residues in an Anti-HIV-1 Env Peptide Synergistically Improves Potency

Michael Y. K. Leung and Fredric S. Cohen*
Department of Molecular Biophysics and Physiology, Rush University Medical Center, Chicago, Illinois

ABSTRACT T-20/Fuzeon/Enfuvirtide (ENF), a peptide inhibitor of HIV-1 infection, targets the grooves created by heptad repeat 2 (HR2) of Env's coiled-coil, but mutants resistant to ENF emerge. In this study, ENF-resistant mutants—V38A, N43D, N43D/S138A, Q40H/L45M—were combined with modified inhibitory peptides to identify what we believe to be novel ways to improve peptide efficacy. V38A did not substantially reduce infectivity, but was relatively resistant to inhibitory peptides. N43D was more resistant to inhibitory peptides than wild-type, but infectivity was reduced. The additional mutation S138A (N43D/S138A) increased infectivity and further reduced peptide inhibitory potency. It is concluded that S138A increased binding of HR2/ENF into grooves and that S138A compensated for electrostatic repulsion between N43D and HR2. The six-helix bundle structure indicated that E148A should increase hydrophobic interactions between the coiled-coil and peptide. Importantly, the modifications S138A and E148A in the same peptide retained potency against ENF-escape mutants. The double mutant's increase in potency was greater than the increases from the sum of S138A and E148A individually, showing that these two altered residues synergistically contributed to peptide binding. Isothermal titration calorimetry established that hydrophobic substitutions at positions S138 and E148 improved potency of inhibitory peptides against escape mutants by increasing enthalpic release of energy upon peptide binding.

## INTRODUCTION

Human immunodeficiency virus type 1 (HIV-1) is the major causative agent of the AIDS pandemic. The protein that mediates fusion of the virus to cells, HIV-1 Env, is a homotrimer; each monomer consists of two noncovalently bound subunits: gp120 and gp41. The fusion subunit, gp41, contains a six-helix bundle (6HB) that consists of a trimer of hairpins in its final—but not its initial—state. Before the formation of the 6HB, gp41 folds into a prehairpin structure. In this structure, a trimeric coiled-coil (composed of three heptad repeats, one per monomer, each designated HR1) has three grooves exposed. During the formation of this prehairpin, hydrophobic fusion peptides within gp41 become anchored in the target cell membrane. After the prehairpin has formed, three other heptad repeats (HR2) insert into the three grooves of the coiled-coil to complete the 6HB. Hydrophobic amino-acid residues of HR2 provide the key interactions with the hydrophobic grooves to form the stable 6HB (1,2). Steps that lead to bundle formation drive both formation and enlargement of the fusion pore (3,4), allowing delivery of the viral core into the cytoplasm of the target cell, completing the entry process (5). Preventing bundle formation blocks viral infection.

Synthetic N-peptides that cover some or all of HR1 can be used to create an experimental model of the natural coiled-coil. Synthetic peptides that include the amino-acid sequence of HR2 (such as C34) prevent viral infection by binding to the grooves of the triple-stranded coiled-coil, thereby blocking binding of the natural HR2 to these sites (1,6). One such peptide, T20/Fuzeon/Enfuvirtide (ENF), has been clinically approved by the FDA for therapeutic use against HIV-1 (7). HIV-1 Env rapidly mutates, and it has been found that the efficacy of ENF treatment for some patients is reduced over time, due to the accumulation of HIV-1 mutants that are resistant to the blocking effects of ENF. This selection of escape mutants can occur quickly, and these mutants can become prominent after only a few weeks of ENF therapy (8–10). Analysis of ENF-resistant isolates shows that the relevant mutations always occur within residues 36–45 of HR1 (11).

As of this writing, as cited by the International AIDS Society in 2009, 16 ENF-resistant mutants have been definitively identified (12–18); of those tested, all have a reduced affinity for ENF; their gp41 mutants still fold into a 6HB, even in the presence of a high concentration of ENF (19). The coiled-coils of the mutated trimers should have reduced affinity for the natural HR2, and in fact, the escape mutants are less infectious than wild-type (WT) (20). Although the mechanisms that viruses use to escape inhibitory peptides are clearly of importance, why these mutations confer ENF resistance is not molecularly understood. Mutations could reduce ENF binding for multiple reasons, including disruption of packing, electrostatic interactions, hydrophobic effects, and/or entropic contributions.

The escape mutant N43D can become a significant fraction of the HIV-1 load in patients treated with ENF. Over time, a second mutation, S138A, can develop on gp41 carrying N43D. The S138A mutation does not appear unless N43D is present. The double mutant N43D/S138A has greater resistance to ENF than the single N43D escape mutant (18).

*Submitted November 27, 2010, and accepted for publication February 28, 2011.*

*Correspondence: fcohen@rush.edu

Editor: Thomas J. McIntosh.


0006-3495/11/04/1960/9 $2.00

doi: 10.1016/j.bpj.2011.02.053

Several efforts have been directed toward developing peptides that retain potency against ENF-escape mutants. These studies have generally been based on the fact that ENF is a random coil in solution, but becomes $\alpha$-helical after binding to coiled-coils (21). Inhibitory peptides have been modified by varied means, with the goal of increasing the $\alpha$-helicity of inhibitory peptides in solution (22–24), to reduce the entropic penalty for free energy of binding. In this study, we have employed an alternate approach. From inspection of the crystal structure and homology modeling, we made changes in an inhibitory peptide that should increase interactions of the peptide with the grooves of HR1. This would improve the enthalpic, rather than the entropic, contribution to free energy of binding. We show that a peptide with two alterations, each of which separately improves interactions, increases inhibitory potency synergistically, and retains potency against common ENF-escape mutants.

## EXPERIMENTAL PROCEDURES

### Reagents and cells

The X4 $HIV_{HXB2}$ envelope expression plasmid E7-HXBc2(IIIexE7pA-Kpn2′), which we refer to as pHXB2, was provided by Dr. J. A. Nunberg (University of Montana, Missoula, MT). HeLa-JC5.3 cells (25) were obtained from Dr. D. Kabat (OHSU, Portland, Oregon). RPMI-1640 and fetal bovine serum were purchased from Hyclone (Logan, UT). All C-peptides were synthesized by Genemed Synthesis (San Antonio, TX). Sequences with residues that were altered from those of C34 are shown in bold and underlined as follows:

C34: WMEWDREINNYTSLIHSLIEESQNQQEKNEQELL.
C-S138A: WMEWDREINNYTSLIHSLIEE**A**QNQQEKNEQELL.
C-E148A: WMEWDREINNYTSLIHSLIEESQNQQEKN**A**QELL.
C-S138A/E148A: WMEWDREINNYTSLIHSLIEE**A**QNQQEKN**A**QELL.
C-S138Abu/E148A: WMEWDREINNYTSLIHSLIEE**Abu**QNQQEKN**A**QELL.

N36 and N46 have the amino-acid sequences:

N36: ……..SGIVQQQNNLLRAIEAQQHLLQLTVWGIKQLQARIL.
N46: ……..TLTVQARQLLSGIVQQQNNLLRAIEAQQHLLQLTVWGIKQLQARIL.

### Homology models for the structure of the 6-helix bundle of gp41 mutants resistant to ENF

Homology models were generated using the Swiss-PDB-viewer. The structure for the S138A mutation was generated by using the crystal structure of HIV-1 gp41 6HB (pdb:1F23) as a template. Using the NMR structure of the 6HB of SIV gp41 (pdb:2EZO) as a template yielded the same result. Residue E148 is not part of 1F23, but is included in 2EZO, and so the structure for E148A was generated by using 2EZO as a template. The final homology model for a mutated residue was generated by energy minimization which was executed for all atoms. The side chains of amino acids are displayed in figures as either stick or van der Waals structures. In figures, atoms are colored according to the Corey/Pauling/Koltun scheme: N is blue, O is red, C is white, and S is yellow.

### Site-directed mutagenesis

The pHXB2 plasmid was used to express HIV Env (HXB2 requires CXCR4 for infection). A double PCR method was used to generate mutants of this envelope protein. In the first round of PCR, forward and reverse primers (2 $\mu$g of each) were added to 96 $\mu$L of a PCR cocktail containing 250 ng of plasmid DNA, 3 units of *Pfu* DNA polymerase, and 1 unit of *Taq*2000 DNA polymerase (Stratagene, La Jolla, CA). The forward primer carried the *Nhe*I site with the sequence derived from 1610-1636 of pHXB2; the reverse primer contained the mutated codon and had ~40 nucleotides flanking both sides of the codon. The product of first round of PCR was used as the forward primer in the second round of PCR. The reverse primer for the second PCR carried the *Bam*HI site with a sequence derived from 2810-2838 of pHXB2. The first PCR consisted of 33 cycles of denaturing at 95°C for 30 s, annealing at 55°C for 30 s, and extending at 72°C for 3 min. The second PCR used the same cycling protocol, but with a 4 min extension time. The PCR product containing the mutant codon was ligated into the *Nhe*I and *Bam*HI sites of pHXB2.

### Generation of HIV/HIV pseudotyped virus

The day before transfection, HEK293T cells were seeded, in 6 $cm^2$ dishes, at $5.5 \times 10^5$ cells in 5 mL of RPMI-1640 culture medium supplemented with 10% fetal bovine serum. For transfection, 15 $\mu$g each of pHXB2 and pNL4-3.Luc.R-E- (National Institutes of Health AIDS Research and Reference Reagent Program, Bethesda, MD) were added to the HEK293T cells by a standard calcium phosphate method. The culture supernatant contained pseudotyped viruses; it was collected two days after transfection and passed through a 0.45 $\mu$m filter.

### Infectivity assay

A collected supernatant (320 $\mu$L) that contained virions was added to 50 $\mu$L of RPMI-1640 + 10% FCS bathing $2 \times 10^5$ HeLa-JC5.3 cells/mL (25) within a well of a multi-well plate (CulturPlate 96; Perkin Elmer, Wellesley, MA). The virus-cell mixture was cultured for two days before performing a luciferase assay (Promega, Madison, WI). The luciferase reading was normalized by the p24 level in the virus-containing medium. The level of p24 was determined by ELISA (Perkin Elmer).

### Isothermal titration calorimetry

We performed isothermal titration calorimetry (ITC) measurements with a high-sensitivity VP-ITC instrument (MicroCal, Northampton, MA). Peptides were dissolved in 50 mM $NaHPO_4$ and 50 mM NaCl. We titrated the solution to pH 8.0 because C-S138A/E148A was not soluble at pH 7.4 and lower. All solutions were degassed under vacuum just before use. Multiple injections of 150 $\mu$M of C34 or C-S138A/E148A were delivered into a reaction cell, maintained at 25°C, containing 5 $\mu$M N46 (26). The solution was stirred at 300 rpm; the time between injections was 5 min. The heats of dilution were determined by injecting C34 or C-S138A/E148A into the sodium phosphate buffer in the absence of N46. The thermodynamic parameters characterizing binding of C34 or C-S138A/E148A to N46 were determined with the MicroCal Origin software (Ver. 7.0), using a model that assumes that an N46 trimer contains three independent binding sites for a C-peptide.

## RESULTS

### Rationale

We utilized the crystal structure of the 6HB of WT HIV-1 Env as a template to investigate how the escape mutations alter the bundle (pdb:1F23). In the three-dimensional structure, WT residue N43 of HR1 is physically closer to E137 than to S138 of HR2. Because the electrically neutral

asparagine (N43) and the negatively charged aspartic acid (N43D) are virtually the same size, differing by only one hydrogen atom, the mutation N43D should not alter the packing of the 6HB for geometrical reasons. Rather, the mutation N43D should reduce the adhesion between HR1 and HR2 (or ENF) because N43D should electrostatically repel residue E137.

Previous investigators inspected a single monomer within the trimeric crystal structure of the 6HB of HIV-1 Env and concluded that the S138 side chain interacts with Q40 and L45 (18). We examined the crystal structure while viewing the full trimer and found that S138 fits into a hydrophobic pocket formed by N43, L44, L45, A46, and I48 of HR1 (Fig. 1 *A* shows the pocket, Fig. 1 *B* illustrates the position of S138 within the pocket, and Fig. 1 *C* shows that the mutation S138A is well positioned within the pocket). Q40 is not part of the pocket and is separated from S138 by ~1.3 nm. Thus, Q40 should not significantly interact with S138, contrary to prior conclusions drawn by others. Identification of the hydrophobic pocket is critical for understanding how S138 interacts with the grooves created by HR1 (27). Based on size and shape, Ala should fit into the hydrophobic pocket as well as Ser does, and so the substitution of Ala for Ser at position 138 should increase the adhesion between HR1 and HR2. That is, the naturally occurring S138 may not be optimal for binding into grooves. By this line of reasoning, the second mutation S138A (yielding N43D/S138A) is favorable for infection in the presence of ENF because the greater hydrophobicity of alanine at position 138 aids hydrophobic interactions between HR1 and HR2 (Fig. 1 *D*, *left*, shows WT and *right* shows N43D).

The NMR structure of SIV gp41 covers a longer stretch than the crystal structures of HIV-1 gp41, so we used the NMR structure (2EZO) of the 6HB to locate unidentified positions where changes in an HR2 peptide could improve inhibitory potency. We found that E148 is in close proximity to L33 and S35 (Fig. 2). Since completing this study, a crystal structure covering the NMR structure has been published (28). The two structures are quite similar, and our interpretations are consistent with both. So an inhibitory peptide containing E148A should have a more favored hydrophobic interaction with L33 and less electrostatic repulsion with S35, thereby increasing the peptide's potency against infection.

## Effect of mutation on viral infectivity

We created several pseudotyped viruses that carried known ENF-resistant mutations and determined their levels of infectivity (Fig. 3) and of inhibition by C34. We used C34 as our test peptide, rather than ENF, because C34 is easier and less costly to synthesize (21); more reversibly binds to the grooves of the trimeric coiled-coil; shows much less nonspecific binding to surfaces (4); and is more potent in blocking infection and fusion (29). Although C34 is not useful for clinical purposes because it is quickly cleared by the body (30), C34 is superior to ENF for basic experimental studies.

The naturally occurring escape mutant V38A was almost as infectious as WT (Fig. 3), as reported by others (29,31,32), and C34 was approximately four-times less potent against this mutant than against WT (Fig. 4, Table 1). The escape mutant N43D exhibited low infectivity (Fig. 3), probably because of greater electrostatic repulsion of HR2. We found that N43D is more resistant against C34 (Fig. 4, Table 1). Our introduction of a second mutation to create

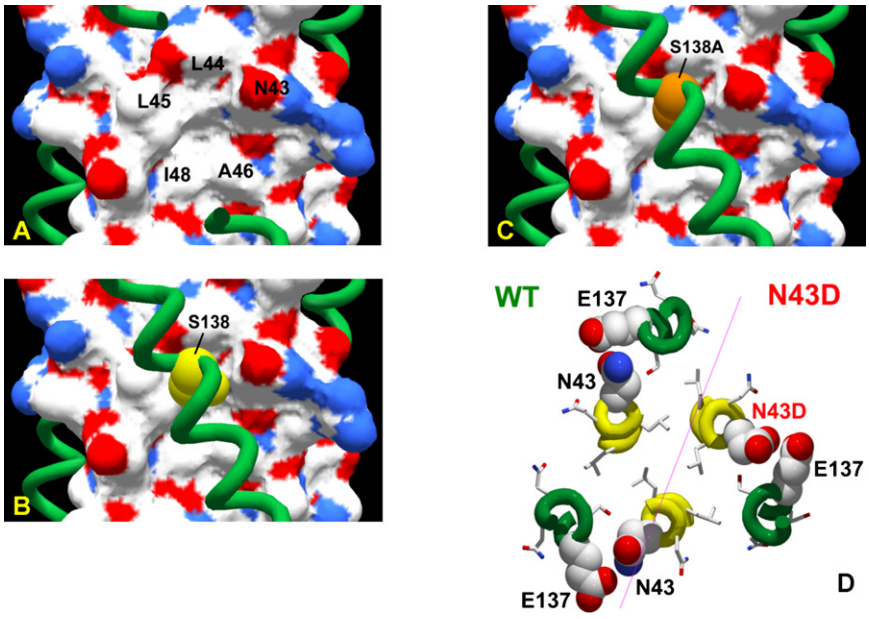


FIGURE 1 Protein homology models of the 6HB for the mutations S138A and N43D. (*A*) The hydrophobic pocket—formed by N43, L44, L45, A46 and I48—that interacts with S138 and S138A, is shown within the molecular surface of a HR1 trimer. HR2 is shown as a green helix. (*B*) The positioning of S138 (the serine side chain is *yellow*) within the pocket is shown. (*C*) The alanine side chain (shown in *orange*) for the mutation fits well into the pocket. (*D*) The consequences of the mutation N43D on the structure of the 6HB. This panel is divided into two parts; the left shows WT and the right shows N43D. N43 and N43D are in close apposition to E137. The mutation N43D only changes the side chain by one Dalton, so size changes are irrelevant. But the net negative charge introduces a electrostatic repulsion between N43 and E137 which should reduce the affinity of HR1 for HR2/ENF. (*Yellow*) HR1 helices. (*Green*) HR2 helices.

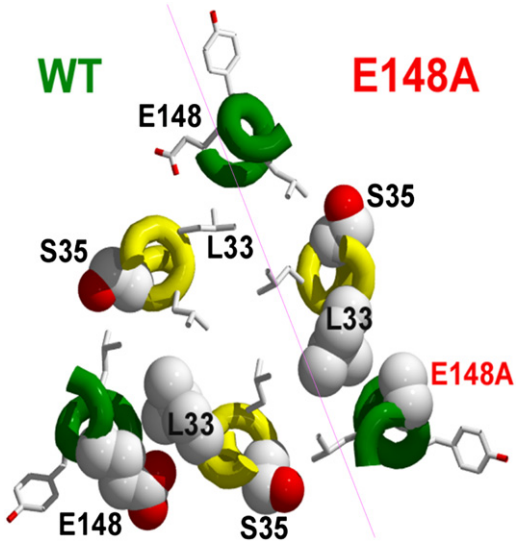


FIGURE 2 The consequences of the mutation E148A on the 6HB structure. (*Left*) WT. (*Right*) Mutant. E148 abuts L33 and is close to S35. The E to A substitution should improve the hydrophobic interaction with L33 and reduce electrostatic repulsion with S35.

N43D/S138A increased infectivity by almost 100% (Fig. 3). It also reduced the potency of C34 by more than a factor of 10 as compared to WT and a factor of five compared to N43D (Fig. 4). Introducing the S138A mutation alone did not greatly affect infectivity. We found that the mutant E148A was somewhat less infectious than WT.

## Interactions between HR1 and HR2 are not optimal in WT

Because Env undergoes large-scale conformational changes during membrane fusion, an altered HR2 could modify many steps, in addition to HR2 packing, in fusion and viral infectivity, and it would not be possible to pinpoint all these

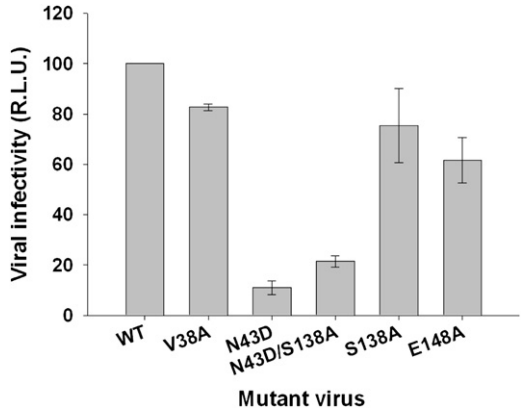


FIGURE 3 Extents of viral infectivity for ENF escape mutants. Infectivity was normalized by the p24 level for that mutant. The means were determined from the averages of three separate experiments. Error bars are mean ± SE.

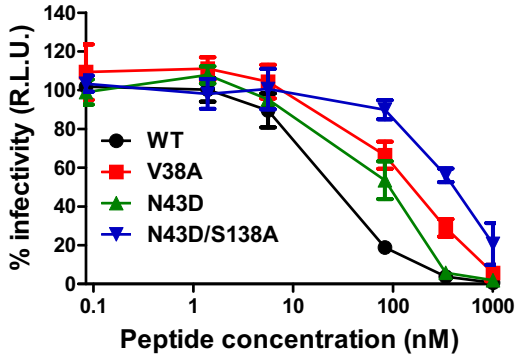


FIGURE 4 Inhibitory potency of C34 against virions pseudotyped with Env proteins that are escape mutants against ENF.

interactions. Altered peptides, however, provide a focused, specific way to study packing into grooves. To explore adhesions between HR1 and HR2 in bundle formation, peptides with the sequence of C34 were synthesized, but with an alanine placed at selected positions.

We used a C34 analog corresponding to S138A (position 22 of C34) which we denote as C-S138A; an analog corresponding to E148A (denoted C-E148A); and an analog corresponding to mutations at both positions (C-S138A/E148A). We found that there were only small variations in the potency of these peptides in inhibiting infection by WT (Fig. 5 *A*, Table 1). Within this range, C-S138A/E148A was the most potent of the four peptides. To further differentiate the potency of the inhibitory peptides, we tested them against several mutant pseudovirions (Table 1): V38A (Fig. 5 *B*), N43D (Fig. 5 *C*), and N43D/S138A (Fig. 5 *D*).

It is striking that for all the mutant pseudovirions, the potency of the peptides always followed the same sequence: C-S138A/E148A > C-S138A > C-E148A > C34. We also compared the potency of C-S138A/E148A and C34 against the double mutant pseudovirus Q40H/L45M. Here too, C-S138A/E148A was dramatically more potent that C34 (Table 1). It is clear that the alteration S138A or E148A in C34 significantly enhanced inhibitory potency of the

**TABLE 1 Antiviral activity of C34 modified peptides against HIV-1 ENF resistant mutants**

| | $IC_{50}$ (nM) | | | | |
|---|---|---|---|---|---|
| Pseudotyped virus | C34 | C-E148A | C-S138A | C-S138A/E148A | C-S138Abu/E148A |
| WT | 40 (1) | 35 (1.1) | 41 (1) | 32 (1.3) | 29 (1.4) |
| V38A | 155 (1) | 110 (1.4) | 57 (2.7) | 23 (6.7) | / |
| N43D | 77 (1) | 78 (1) | 30 (2.6) | 11 (7) | 8 (9.6) |
| N43D/S138A | 408 (1) | 331 (1.2) | 140 (2.9) | 37 (11) | 26.5 (15.4) |
| Q40H/L45M | >6000 (1) | / | / | 199 (>30) | / |

Viral infectivity was determined with a luciferase assay. The ratio of the $IC_{50}$ of C34 relative to each modified peptide is shown in parentheses. The value of $IC_{50}$ for C-S138Abu/E148A against V38A was not determined. WT, wild-type.

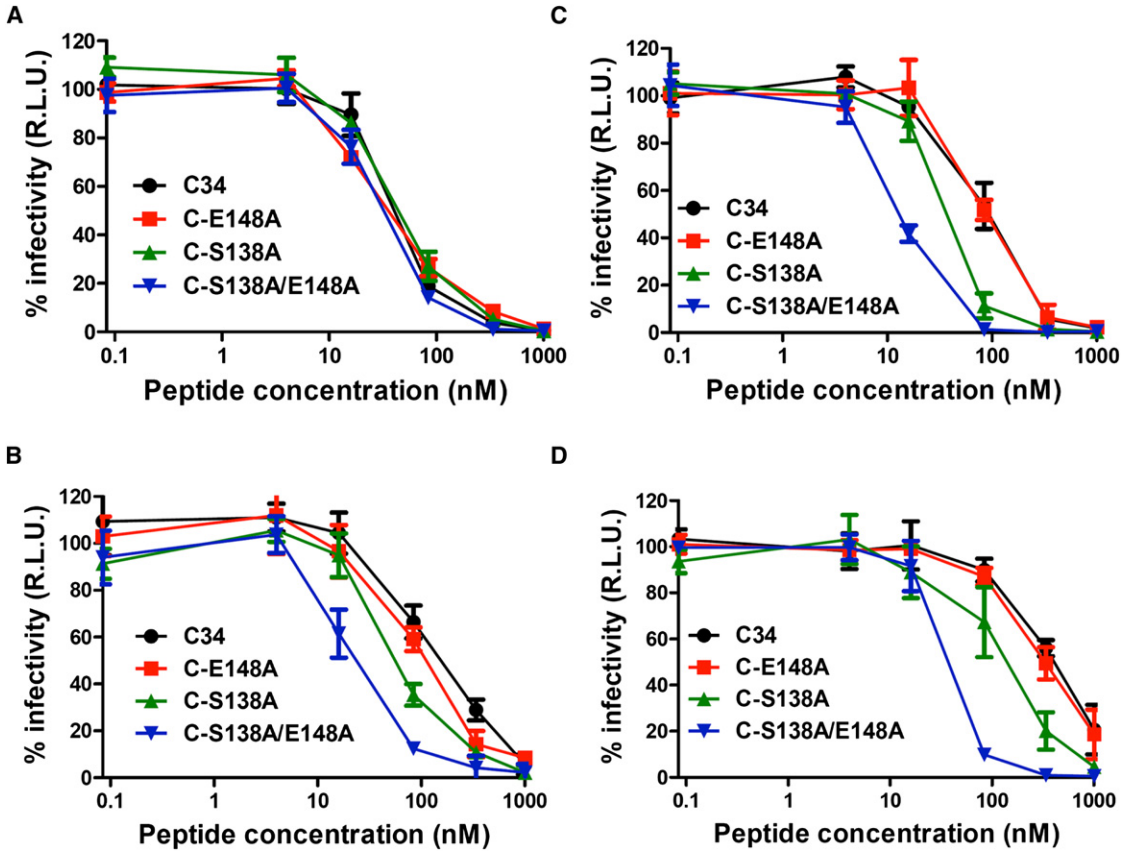


FIGURE 5 The inhibitory potency of pseudotyped viruses against C34 and analogs. (*A*) WT Env, (*B*) V38A Env, (*C*) N43D Env, and (*D*) N43D/S138A Env. The doubly mutated peptide was the most potent inhibitory peptide for all viruses tested; C34 was the least potent.

peptides against ENF-escape mutants. The decrease in $IC_{50}$ of C-S138A/E148A compared to that for both C-S138A and C-E148A is much greater than that expected for additive effects, strongly indicating that packing of S138 and E148 into grooves is synergistic, rather than independent.

Because the improvement in peptide efficacy at position S138 should be due to the greater hydrophobicity of Ala as compared to Ser, we switched position 138 of C34 to the synthetic amino acid, $\alpha$-aminobutyric acid (Abu). Abu has an ethyl side chain that is more hydrophobic than the hydroxylmethyl side chain of Ser and is comparable in size (albeit slightly larger) (Fig. 6 *A*). We compared the potency of the peptide which has S138Abu and E148A (C-S138Abu/E148A) against C-S138A/E148A as well as the other altered peptides. C-S138Abu/E148A displayed the highest inhibitory potency against both N43D (Fig. 6 *B*) and N43D/S138A (Fig. 6 *C*), the two mutated pseudovirions that we tested (Table 1). The greater hydrophobicity of the ethyl side chain was sufficient to make C-S138Abu/E148A approximately one-order-of-magnitude more potent against the N43D pseudovirion than C34. But C-S138Abu/E148A was only somewhat more potent than C-S138A/E148A. The greater relative potency of C-S138Abu/E148A compared to the other two peptides was more pronounced for the N43D/S138A pseudovirion (Table 1).

## Helicity of peptides and stability of the bundle

C34 is unstructured in solution, but becomes $\alpha$-helical upon binding to a groove of the triple-stranded coiled-coil ((33), Lu). Ala favors the formation of $\alpha$-helices (34), so improved inhibitory potency of the S138A and E148A modifications (separately or together) in the peptide may not have occurred through promotion of more favorable interactions with the grooves of HR1, but rather because of an increase in helicity of the peptide in solution. Measuring the CD spectra of the peptides, we found that they all have similar helical content in solution: between 3% and 4% (see Fig. S1 in the Supporting Material). In fact, the helicity of C34 is somewhat higher than that of the modified peptides, even though the modified peptides are the more potent. The invariance of helicity shows the modifications did not change the configurational order of the peptide. But other configurations, such as waters of hydration, could be altered.

A greater affinity of an HR2 peptide for the coiled-coil created by HR1 peptides would yield higher bundle stability.

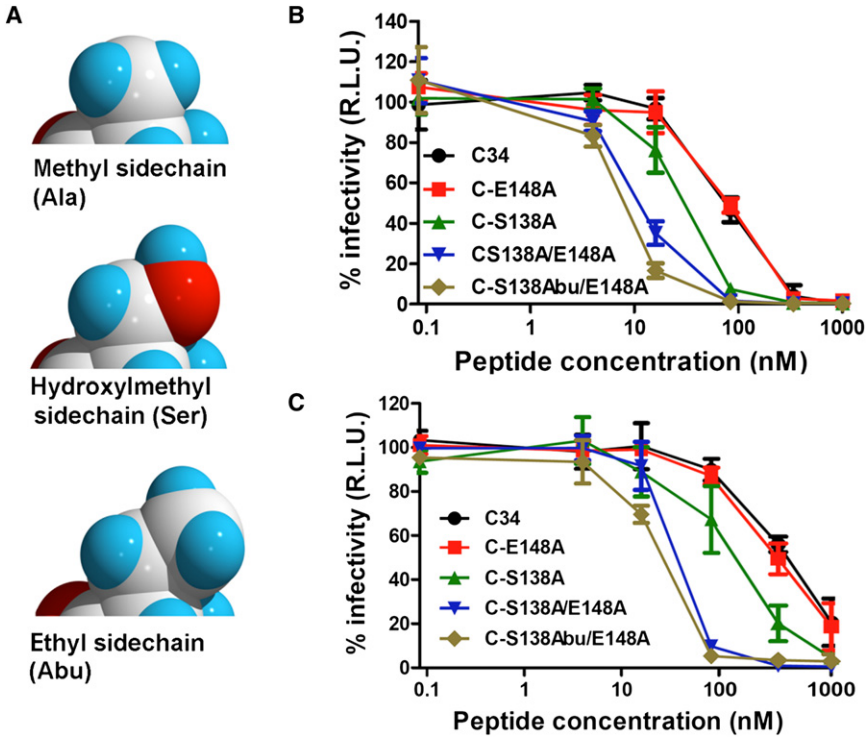


FIGURE 6 Inhibition of infection by C34 and modified peptides for virus pseudotyped with N43D and N43D/S138A. (*A*) The methyl side chain of alanine, the hydroxylmethyl side chain of serine, and the ethyl side chain of α-aminobutyric acid are shown. The size and shape of an ethyl side chain closely resemble that of hydroxylmethyl, but it is more hydrophobic. (*B*) Inhibition curves of peptides against N43D pseudotyped virus. (*C*) Inhibition curves for N43D/S138A. Replacing serine by the more hydrophobic α-aminobutyric acid increased peptide potency.

We measured thermal unfolding transition/melting temperatures ($T_m$ values) of bundles formed by HR1 and HR2 peptides to assess bundle stability. We used N36 as the HR1 peptide, used WT and our modified C34 peptides as the HR2 peptides, and measured $T_m$ for the resulting 6HBs. This yielded measurable values of $T_m$ without the need to add denaturants (e.g., guanidinium chloride). (In contrast, using N46 and C34 led to a 6HB that could not be melted without adding a denaturant.) The order of the values of $T_m$ was the same as the general order for potency of inhibition by the peptides for viral infection: C-S138Abu/E148A > C-S138A/E148A > C-S138A> C-E148A > C34 (Table 2). However, for virions with mutations corresponding to these peptide positions, infectivity did not follow this pattern (Fig. 3). Because inhibitory peptides should be specific in blocking bundle formation, their order of inhibition should be a reasonably direct measure of effect of mutation on bundle formation.

**TABLE 2 Thermal unfolding transition temperature ($T_m$) of 6HB complexes between N36 and variants of C34**

| Six-helix bundle complex | $T_m$ (°C) |
|---|---|
| N36, C34 | 39 |
| N36, C-E148A | 41 |
| N36, C-S138A | 46 |
| N36, C-S138A/E148A | 48 |
| N36, C-S138Abu/E148A | 49 |

## Enthalpic and entropic contributions to the free energy of binding

We performed ITC measurements to determine the change in enthalpy upon peptide binding and to calculate the corresponding changes in free energy and entropy. We compared binding of WT C34 and C-S138A/E148A to N46 because these two C-peptides showed the greatest difference in potency of inhibiting infection. As is obvious from the raw data (Fig. 7, *upper panels*), binding of the double mutant reaches equilibrium at much lower concentrations than binding of C34. This is reflected in the binding curves (Fig. 7, *lower panels*). Quantitatively, the binding affinity is significantly greater for the double mutant: under our conditions, the association constant K is $4.5 \times 10^6$ $M^{-1}$ for the double mutant and only $6 \times 10^5$ $M^{-1}$ for C34 (Table 3). The change in enthalpy of binding was appreciably different for the two peptides, 5.2 kcal/mol more favorable for C-S138A/E148A. This was partially compensated by a 3.5 kcal/mol more favorable entropic contribution to binding for C34. In conclusion, C-S138A/E148A is a more potent inhibitory peptide than C34 because it binds more avidly to the grooves of HR1 than does C34, and does so because it has a greater enthalpic release of energy upon binding.

The entropy change upon binding was less favorable for C-S138A/E148A than for C34. It has been found by others that even much larger changes in entropy of binding of C34 occur for single alterations of the N-peptide, N36 (26).

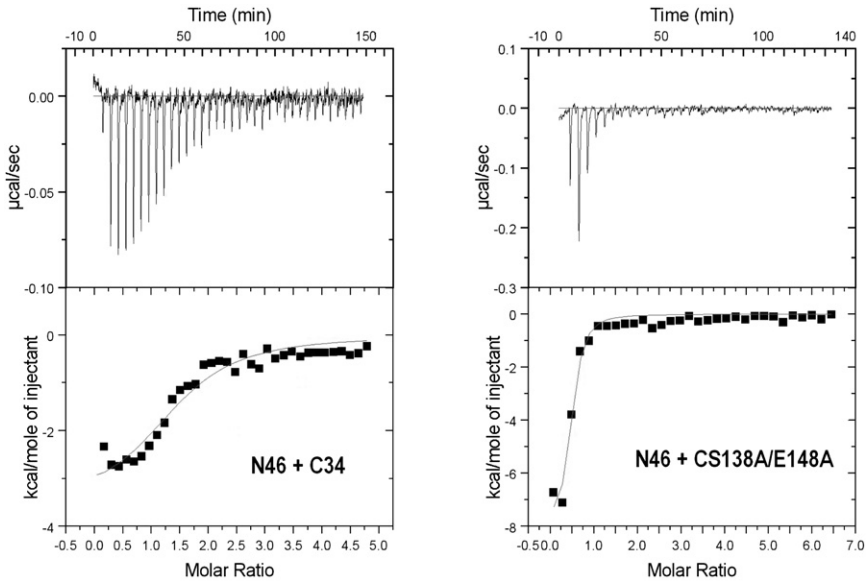


FIGURE 7 ITC measurements of C34 (*left*) and C-S138A/E148A (*right*) binding to N46. (*Upper panels*) Raw thermographs. (*Lower panels*) Fitted binding isotherms. The ordinates of the upper panels are the heat flows (power) resulting from each injection; the ordinates of the lower panels are the integrated areas over time of each spike of the corresponding upper panel, yielding the heat (enthalpy) exchanged after each injection. The abscissas of the lower panels are the molar ratios of the indicated C-peptide/ N46. A quantity of 5 $\mu$M N46 was initially added to the cuvette. The $\Delta G$ of C-S138A/E148A binding is ~1 kcal mol$^{-1}$ more negative than that of C34 binding, and is almost entirely enthalpy-driven. $\Delta H$ (see Table 3) contributes ~90% of the $\Delta G$ for C-138A/E148A, but only 44% of $\Delta G$ for C34. Note that the scales are different for C34 and C-S138A/E148A.

Possible molecular reasons for the less favorable entropic contribution for S138A/E148A include the reduced number of carbon bonds for rotation in the altered side chains (particularly for Ala as compared to Glu), less freedom of the mutated peptide once it is bound to grooves of the coiled-coil (because Ala fits better into the grooves than the natural amino acids), and altered configurations of water surrounding unbound peptides caused by hydrophobic alanines.

## DISCUSSION

The order for the potency of the peptides in preventing viral infection and the stability of the bundles (as measured by $T_m$) they form with an HR1 peptide (N36) followed the same sequence: C-S138Abu/E148A > C-S138A/E148A > C-S138A > C-E148A > C34. Although bundle stability does not correlate with either extents or kinetics of fusion (35–37), we have now found that stability does correlate with the ability of a peptide to inhibit fusion. We consider it notable that the order of inhibition by the peptides we used is accounted for by the interactions inferred from the crystal structure (see Rationale, above). It has recently been shown that the qualitative order of inhibitory potency for a set of ENF analogs also follows alterations in interactions that were deduced, by the same logic we employed, from the crystal structure (31).

**TABLE 3 Thermodynamic parameters of C34 and C-S138A/E148A binding to N46**

| | $\Delta H$ (kcal mol$^{-1}$) | $T\Delta S$ (kcal mol$^{-1}$) | $\Delta G$ (kcal mol$^{-1}$) | $K$ (M$^{-1}$) |
|---|---|---|---|---|
| C34 | −3.5 | 4.4 | −7.9 | $6.6 \times 10^5$ |
| C-S138A/E148A | −8.2 | 0.9 | −9.1 | $4.5 \times 10^6$ |

### The appearance of escape mutants

The mutation V38A is frequently found in patients undergoing ENF treatment. This is undoubtedly related to the decreased potency of ENF against this mutant (19) and the fact that the mutant virus retains >80% of the infectivity of WT (Fig. 3). The propagation advantage of N43D should rest on its increased resistance to ENF over WT (38). We infer from the crystal structure that the mutated N43D virus is electrostatically repelled from E137, and this could account for its reduced infectivity. The compensatory mutation S138A that appears after N43D is selected (i.e., N43D/S138A) in the presence of ENF partially restores infectivity, but it is still far short of the infectivity of WT. The greater hydrophobic interactions between S138A and the hydrophobic pocket, leading to the greater infectivity of the double than the single mutant, should partially—but not completely—offset the increased electrostatic repulsion arising from N43D. The combination of increased infectivity and greater resistance to an inhibitory peptide is probably the reason the mutation S138A arises, during ENF treatment of patients, after the first mutation N43D appears.

Inspection of the bundle's crystal structure indicated that changing E148 to alanine would improve the inhibitory efficacy of the peptide because of the reduction in charge and the increase in hydrophobicity. Reduced infectivity of E148A, despite these more favored interactions, indicates that mutations of residues in the bundle region affects processes other than formation of the bundle itself—perhaps including viral assembly, protein folding, conformations of

intermediates, or compatibility with other domains of gp41. C-E148A was somewhat more effective than C34 in blocking fusion. C-S138A/E148A, on the other hand, was considerably more potent than C34, C-S138A, or C-E148A in blocking infection by WT and the viral mutants. It might thus be thought that this double mutation would appear in the presence of ENF. However, this has not been reported, and BLAST software did not show protein sequences containing S138A and E148A in HIV-1 Env.

The modified C34 peptides had varied potencies against all the mutant virions, but all the peptides had the same inhibitory activity against WT virus. For a peptide to inhibit fusion, it must bind to prehairpin structures of gp41. This can only occur while the virions are still bound to the plasma membrane, before their endocytic internalization (5,39). It is possible that WT virus is internalized faster than the mutants, and binding of the peptides is limited by this internalization.

### Thermodynamic reasons for improved peptide potency

Unbound inhibitory peptides reconfigure from a less ordered to a more ordered structure upon associating with HR1. Greater order leads to a decrease in entropy, and because this is energetically unfavorable, it must be compensated by a greater favorable decrease in enthalpy if the peptide is to bind (40,41). Investigators have introduced covalent constraints (42) or intramolecular salt bridges (23,24,42) to increase ENF helicity in solution. These modifications increased the inhibitory potency of the peptides, demonstrating that reducing the entropic penalties of binding improves efficacy of the peptides. Our modifications, on the other hand, did not affect helicity of the peptides in solution (Fig. 7), and so increased potencies of the peptides would likely be caused by more favorable enthalpic contributions to binding. The results of our ITC experiments confirm this expectation. A more favored enthalpy is equivalent to increased adhesive forces between the modified peptides and HR1 grooves. Based on the crystal structure, more favorable hydrophobic interactions with the HR1 grooves are responsible for the greater adhesive forces (27).

For bundle stability to directly vary with the strength of hydrophobic interactions between HR1 and a peptide, the substitutions should not disfavor geometrical packing of the peptide into the grooves. For C-S138A, Ala's methyl side chain is smaller than the hydroxylmethyl side chain of Ser. Visual inspection of the crystal structure indicates that alanine's methyl group fits very well into the hydrophobic pocket formed by N43, L44, L45, A46, and I48 of HR1 (Fig. 1), possibly better than the hydroxylmethyl side chain serine that normally occupies it. C-E148A should more favorably pack into HR1 grooves than does C34 because it should have a more favorable hydrophobic interaction with L33 than does C34 without causing any geometrical clashes.

The synergistic increase in inhibitory potency of the doubly changed peptides C-S138A/E148A and C-S138Abu/S148A is likely to be a consequence of the two hydrophobic patches created by the substitutions. The distance between the centers of these two patches, separated by three $\alpha$-helical turns, should be ~1.6–1.7 nm. Therefore, a linear chain of approximately six water molecules separates the two hydrophobic patches. The network of H-bonds between water molecules adjacent to a hydrophobic patch will be altered (43), so much (or all) of the H-bond network between the patches should be different from that of bulk water. We propose that the altered H-bond structure intervening between the patches reduces the energy necessary to remove the water molecules separating HR2 from the grooves created by HR1, and this is the direct mechanistic cause of the synergic greater binding.

In this study we have shown that the potency of inhibitory peptides can be improved by designing them to yield greater enthalpic release of energy upon binding. It should be possible to design inhibitory peptides that yield both more favorable entropic and enthalpic contributions to free energy release upon peptide binding to coiled-coils of viral fusion proteins, thus maximizing the potency of peptides in prevention of infection. Our proposed physical principle that nearby hydrophobic patches synergistically improves peptide binding may prove to be a useful and general principle for design of inhibitory peptides to maximize enthalpic energy release upon binding to hydrophobic grooves of coiled-coils. In any case, our finding that the joint alterations S138A and E148A in C34 yield a peptide that retains full inhibitory potency against the tested escape mutants could provide the basis for a second generation of inhibitory peptides, ones that retard the appearance of a large number of escape mutants.

## SUPPORTING MATERIAL

One figure and figure legend are available at http://www.biophysj.org/biophysj/supplemental/S0006-3495(11)00306-7.

We thank Dr. Jaydeep Bardeen for useful conservations regarding thermodynamics of peptide binding. pNL43.Luc.R-E- was obtained through the National Institutes of Health AIDS Research and Reference Reagent Program, Division of AIDS, The National Institute of Allergy and Infectious Diseases, National Institutes of Health.

This work was supported by National Institutes of Health grant No. R01 GM027367.

## REFERENCES

1. Chan, D. C., D. Fass, …, P. S. Kim. 1997. Core structure of gp41 from the HIV envelope glycoprotein. *Cell.* 89:263–273.
2. Weissenhorn, W., A. Dessen, …, D. C. Wiley. 1997. Atomic structure of the ectodomain from HIV-1 gp41. *Nature.* 387:426–430.

3. Markosyan, R. M., F. S. Cohen, and G. B. Melikyan. 2003. HIV-1 envelope proteins complete their folding into six-helix bundles immediately after fusion pore formation. *Mol. Biol. Cell.* 14:926–938.
4. Melikyan, G. B., R. M. Markosyan, …, F. S. Cohen. 2000. Evidence that the transition of HIV-1 gp41 into a six-helix bundle, not the bundle configuration, induces membrane fusion. *J. Cell Biol.* 151:413–423.
5. Miyauchi, K., Y. Kim, …, G. B. Melikyan. 2009. HIV enters cells via endocytosis and dynamin-dependent fusion with endosomes. *Cell.* 137:433–444.
6. Lawless, M. K., S. Barney, …, G. Merutka. 1996. HIV-1 membrane fusion mechanism: structural studies of the interactions between biologically-active peptides from gp41. *Biochemistry.* 35:13697–13708.
7. Robertson, D. 2003. US FDA approves new class of HIV therapeutics. *Nat. Biotechnol.* 21:470–471.
8. Poveda, E., B. Rodés, …, V. Soriano. 2002. Evolution of the gp41 Env region in HIV-infected patients receiving T-20, a fusion inhibitor. *AIDS.* 16:1959–1961.
9. Poveda, E., B. Rodés, …, V. Soriano. 2004. Evolution of genotypic and phenotypic resistance to enfuvirtide in HIV-infected patients experiencing prolonged virologic failure. *J. Med. Virol.* 74:21–28.
10. Pérez-Alvarez, L., R. Carmona, …, R. Nájera. 2006. Long-term monitoring of genotypic and phenotypic resistance to T20 in treated patients infected with HIV-1. *J. Med. Virol.* 78:141–147.
11. Lu, J., S. G. Deeks, …, D. R. Kuritzkes. 2006. Rapid emergence of enfuvirtide resistance in HIV-1-infected patients: results of a clonal analysis. *J. Acquir. Immune Defic. Syndr.* 43:60–64.
12. Greenberg, M. L., and N. Cammack. 2004. Resistance to enfuvirtide, the first HIV fusion inhibitor. *J. Antimicrob. Chemother.* 54:333–340.
13. Marcial, M., J. Lu, …, D. R. Kuritzkes. 2006. Performance of human immunodeficiency virus type 1 gp41 assays for detecting enfuvirtide (T-20) resistance mutations. *J. Clin. Microbiol.* 44:3384–3387.
14. Menzo, S., A. Castagna, …, M. Clementi. 2004. Genotype and phenotype patterns of human immunodeficiency virus type 1 resistance to enfuvirtide during long-term treatment. *Antimicrob. Agents Chemother.* 48:3253–3259.
15. Rimsky, L. T., D. C. Shugars, and T. J. Matthews. 1998. Determinants of human immunodeficiency virus type 1 resistance to gp41-derived inhibitory peptides. *J. Virol.* 72:986–993.
16. Sista, P. R., T. Melby, …, M. L. Greenberg. 2004. Characterization of determinants of genotypic and phenotypic resistance to enfuvirtide in baseline and on-treatment HIV-1 isolates. *AIDS.* 18:1787–1794.
17. Wei, X., J. M. Decker, …, J. C. Kappes. 2002. Emergence of resistant human immunodeficiency virus type 1 in patients receiving fusion inhibitor (T-20) monotherapy. *Antimicrob. Agents Chemother.* 46:1896–1905.
18. Xu, L., A. Pozniak, …, D. Pillay. 2005. Emergence and evolution of enfuvirtide resistance following long-term therapy involves heptad repeat 2 mutations within gp41. *Antimicrob. Agents Chemother.* 49:1113–1119.
19. Mink, M., S. M. Mosier, …, M. L. Greenberg. 2005. Impact of human immunodeficiency virus type 1 gp41 amino acid substitutions selected during enfuvirtide treatment on gp41 binding and antiviral potency of enfuvirtide in vitro. *J. Virol.* 79:12447–12454.
20. Reeves, J. D., F. H. Lee, …, R. W. Doms. 2005. Enfuvirtide resistance mutations: impact on human immunodeficiency virus envelope function, entry inhibitor sensitivity, and virus neutralization. *J. Virol.* 79:4991–4999.
21. Kliger, Y., and Y. Shai. 1997. A leucine zipper-like sequence from the cytoplasmic tail of the HIV-1 envelope glycoprotein binds and perturbs lipid bilayers. *Biochemistry.* 36:5157–5169.
22. Bird, G. H., N. Madani, …, L. D. Walensky. 2010. Hydrocarbon double-stapling remedies the proteolytic instability of a lengthy peptide therapeutic. *Proc. Natl. Acad. Sci. USA.* 107:14093–14098.
23. Dwyer, J. J., K. L. Wilson, …, M. K. Delmedico. 2007. Design of helical, oligomeric HIV-1 fusion inhibitor peptides with potent activity against enfuvirtide-resistant virus. *Proc. Natl. Acad. Sci. USA.* 104:12772–12777.
24. He, Y., Y. Xiao, …, L. Zhang. 2008. Design and evaluation of sifuvirtide, a novel HIV-1 fusion inhibitor. *J. Biol. Chem.* 283:11126–11134.
25. Kuhmann, S. E., E. J. Platt, …, D. Kabat. 2000. Cooperation of multiple CCR5 coreceptors is required for infections by human immunodeficiency virus type 1. *J. Virol.* 74:7005–7015.
26. He, Y., S. Liu, …, S. Jiang. 2007. Conserved residue Lys574 in the cavity of HIV-1 Gp41 coiled-coil domain is critical for six-helix bundle stability and virus entry. *J. Biol. Chem.* 282:25631–25639.
27. Malashkevich, V. N., D. C. Chan, …, P. S. Kim. 1998. Crystal structure of the simian immunodeficiency virus (SIV) gp41 core: conserved helical interactions underlie the broad inhibitory activity of gp41 peptides. *Proc. Natl. Acad. Sci. USA.* 95:9134–9139.
28. Buzon, V., G. Natrajan, …, W. Weissenhorn. 2010. Crystal structure of HIV-1 gp41 including both fusion peptide and membrane proximal external regions. *PLoS Pathog.* 6:e1000880.
29. Nishikawa, H., S. Nakamura, …, M. Matsuoka. 2009. Electrostatically constrained $\alpha$-helical peptide inhibits replication of HIV-1 resistant to enfuvirtide. *Int. J. Biochem. Cell Biol.* 41:891–899.
30. Stoddart, C. A., G. Nault, …, O. Quraishi. 2008. Albumin-conjugated C34 peptide HIV-1 fusion inhibitor: equipotent to C34 and T-20 in vitro with sustained activity in SCID-hu Thy/Liv mice. *J. Biol. Chem.* 283:34045–34052.
31. Eggink, D., J. P. Langedijk, …, R. W. Sanders. 2009. Detailed mechanistic insights into HIV-1 sensitivity to three generations of fusion inhibitors. *J. Biol. Chem.* 284:26941–26950.
32. Garg, H., A. Joshi, and R. Blumenthal. 2009. Altered bystander apoptosis induction and pathogenesis of enfuvirtide-resistant HIV type 1 Env mutants. *AIDS Res. Hum. Retroviruses.* 25:811–817.
33. Kilgore, N. R., K. Salzwedel, …, C. T. Wild. 2003. Direct evidence that C-peptide inhibitors of human immunodeficiency virus type 1 entry bind to the gp41 N-helical domain in receptor-activated viral envelope. *J. Virol.* 77:7669–7672.
34. Rohl, C. A., W. Fiori, and R. L. Baldwin. 1999. Alanine is helix-stabilizing in both template-nucleated and standard peptide helices. *Proc. Natl. Acad. Sci. USA.* 96:3682–3687.
35. Lu, M., M. O. Stoller, …, J. H. Nunberg. 2001. Structural and functional analysis of interhelical interactions in the human immunodeficiency virus type 1 gp41 envelope glycoprotein by alanine-scanning mutagenesis. *J. Virol.* 75:11146–11156.
36. Markosyan, R. M., M. Y. Leung, and F. S. Cohen. 2009. The six-helix bundle of human immunodeficiency virus Env controls pore formation and enlargement and is initiated at residues proximal to the hairpin turn. *J. Virol.* 83:10048–10057.
37. Wang, S., J. York, …, M. Lu. 2002. Interhelical interactions in the gp41 core: implications for activation of HIV-1 membrane fusion. *Biochemistry.* 41:7283–7292.
38. Izumi, K., E. Kodama, …, M. Matsuoka. 2009. Design of peptide-based inhibitors for human immunodeficiency virus type 1 strains resistant to T-20. *J. Biol. Chem.* 284:4914–4920.
39. Miyauchi, K., M. M. Kozlov, and G. B. Melikyan. 2009. Early steps of HIV-1 fusion define the sensitivity to inhibitory peptides that block 6-helix bundle formation. *PLoS Pathog.* 5:e1000585.
40. Lu, M., S. C. Blacklow, and P. S. Kim. 1995. A trimeric structural domain of the HIV-1 transmembrane glycoprotein. *Nat. Struct. Biol.* 2:1075–1082.
41. Judice, J. K., J. Y. Tom, …, R. S. McDowell. 1997. Inhibition of HIV type 1 infectivity by constrained $\alpha$-helical peptides: implications for the viral fusion mechanism. *Proc. Natl. Acad. Sci. USA.* 94:13426–13430.
42. Sia, S. K., P. A. Carr, …, P. S. Kim. 2002. Short constrained peptides that inhibit HIV-1 entry. *Proc. Natl. Acad. Sci. USA.* 99:14664–14669.
43. Baldwin, C. E., R. W. Sanders, …, B. Berkhout. 2004. Emergence of a drug-dependent human immunodeficiency virus type 1 variant during therapy with the T20 fusion inhibitor. *J. Virol.* 78:12428–12437.